Journal of Vibration Engineering & Technologies (2024) 12:19–36
https://doi.org/10.1007/s42417-022-00824-1

ORIGINAL PAPER

A New Conjugate Gradient Method for Moving Force Identification of Vehicle–Bridge System

Chengsheng Luo[1] · Linjun Wang[1,2] · Youxiang Xie[3] · Baojia Chen[1]

Received: 2 July 2022 / Revised: 28 October 2022 / Accepted: 6 December 2022 / Published online: 19 December 2022

Abstract

A new preconditioned modified conjugate gradient algorithm based on improved gradient operator and preconditioned technology is proposed for moving force identification of bridge structure in this paper. First, the moving load identification problem is converted into the problem of solving large-scale linear equations by the time-domain deconvolution technology and modal superposition method. Then the large-scale linear equations problem is transformed into easily solved equivalent problem by preprocessing. Subsequently, it is transformed into an unconstrained linear optimization problem by constructing the corresponding objective function. Finally, the problem is solved by the proposed conjugate gradient method. The innovation of the proposed method lies in two aspects. First, the proposed conjugate gradient method is proved by mathematical theory. Second, before constructing the objective function, the preconditioned technique is utilized to simplify the original problem. A series of numerical simulations are carried out to verify the stability and effectiveness of the proposed approach under 21 kinds of noise levels and 6 different sensor configurations, and its performances are compared with several conjugate gradient methods. The results show that the proposed method can reduce the iteration number, and also ensure the load identification accuracy, which indicates that the proposed method can improve the speed of identification and effectively reduce the cost. Meanwhile, the identification situation of different load components is studied by the frequency spectrum analysis method. It is found that the proposed method is a stable and a reliable identification method for static and low-frequency components, which provides a new idea for dynamic weighing of low-frequency loads on bridges.

Keywords Moving load identification · Gradient method · Preconditioned technology · Frequency component · Frequency spectrum analysis

✉ Linjun Wang
ljwang2006@126.com

Chengsheng Luo
2298154973@qq.com

Youxiang Xie
xieyouxiangxie@126.com

Baojia Chen
cbjia@163.com

[1] Hubei Key Laboratory of Hydroelectric Machinery Design and Maintenance, College of Mechanical and Power Engineering, China Three Gorges University, Yichang 443002, Hubei, People's Republic of China

[2] School of Chemistry, Physics and Mechanical Engineering, Queensland University of Technology, Brisbane, QLD 4001, Australia

[3] College of Science Technology, China Three Gorges University, Yichang 443002, Hubei, People's Republic of China

Introduction

Dynamic information about moving load on the bridge is closely related to structural design, reliability analysis, fault diagnosis, and other engineering problems. In most practical engineering problems, it is difficult or impossible to directly measure moving loads acting on the bridge structure. However, the dynamic responses of the bridge are easier to obtain without damaging the bridge structure, so the load information can be obtained in an indirect way, i.e., moving force identification (MFI). After decades of research by many scholars, a variety of moving load identification methods have been developed. According to different identification methods, it can be divided into direct method, basis function expansion method, regularization method, function approximation method, intelligent calculation method, and so on.

The direct method is mainly based on the basic theory of structural vibration to deduce and establish the mathematical

equation of MFI. Then matrix inverse method or least square method is used to solve the equation directly. For example, Law et al. [1] proposed the time-domain method to identify the moving load on the bridge from the acceleration and bending moment response. Huang et al. [2] transformed the differential equation of bridge structure vibration into the general form of precise integration, and then obtained the precise integration method for MFI. Hou et al. [3] introduced the idea of precise integration method into the symplectic algorithm to establish a symplectic precise integration method for MFI. Liu et al. [4] proposed a new method called time-domain Galerkin method for investigating the structural dynamic load identification problems. Because the MFI is a typical inverse problem, in the case of measurement error or noise interference, the direct method will encounter the problem of ill-conditioned [5], leading to a large deviation in the identification results. Therefore, the direct method is difficult or impossible to be applied in engineering practice.

For the ill-conditioned problem of moving load identification, the regularization methods have been developed by introducing reasonable additional information as the constraint. For example, Qiao et al. [6] used Tikhonov regularization method to overcome the ill-conditioned problem of bridge moving load identification. Based on integer-order Tikhonov regularization technique, Wang et al. [7] proposed a new fractional Tikhonov regularization technique. Subsequently, Liu et al. [8] constructed an improved fractional order filtering factor and proposed an improved fractional order Tikhonov regularization method. Based on singular value decomposition, Chen et al. [9, 10] proposed the truncated generalized singular value decomposition method and piecewise polynomial truncated singular value decomposition method for moving force identification. Chen et al. [11] developed a novel preconditioned least-square QR-factorization method for moving force identification. Based on the Arnoldi process, Krylov subspace method and generalized minimal residual method, Chen et al. [12] proposed a preconditioned range restricted generalized minimal residual method for moving force identification. Based on sparse regularization technique, Pan et al. [13] proposed a novel moving load identification method. Qiao et al. [14] developed a general sparse regularization method based on minimizing l1-norm of the coefficient vector of basis functions. He et al. [15] proposed a novel modified regularization method to solve the ill-posed problem and mitigate the error propagation of random dynamic loads identification. Feng et al. [16] proposed a novel sparse Kalman filter recursive algorithm to localize and reconstruct the forces in time domain. Based on the redundant concatenated dictionary and weighted-norm regularization method, Wang et al. [17] proposed a hybrid method for MFI. Regularization methods are widely studied because they can improve the ill-conditioned problem of inverse problems, but the constraints introduced by regularization method need to be determined in advance. The regularization parameter plays a role in regulating the constraints. If the regularization parameter is too large, it will lead to excessive constraints; if it is too small, it cannot improve the ill-condition of the inverse problem. Therefore, regularization parameters should be selected reasonably according to practical engineering problems, which are the shortcomings of the regularization method.

The main idea of the basis function expansion method is to expand the unknown moving load using the known function, and transform the problem of load identification into the problem of selecting the basis function coefficient. For example, Qiao et al. [18] proposed an efficient basis function expansion method based on wavelet multi-resolution analysis using cubic B-spline scaling functions as basis functions. Qiao et al. [19] developed a regularized cubic B-spline collocation method for identifying the impact force time history, which overcomes the deficiency of the ill-posed problem. Qiao et al. [20] proposed a novel method based on the discrete cosine transform in the time domain for force identification, which overcomes the deficiency of the ill-posedness of the transfer matrix. Liu et al. [21] proposed an analytical method to identify dynamic loads acting on stochastic structures based on the Gegenbauer polynomial expansion theory and regularization method, and also investigated the parallelotope-formed evidence theory model [22]. There are two key points in identifying moving loads by the basis function method: one is the selection of load basis function type and the other one is the selection of the number of basis function. In fact, the basis function expansion method is a special regularization method.

The main idea of the function approximation method is to use the known basis function to fit the deflection of the measured point, and then obtain the velocity and acceleration from the deflection differentiation. Then the acceleration, velocity, and displacement are substituted into the dynamic equation of the structure to identify the load acting on the bridge. For example, Yuan et al. [23] used the polynomial function, trigonometric function, and their combination to approximate the deflection of measured points. Jiang et al. [24] proposed a cubic spline curve fitting method to identify the moving load of the bridge. However, the identification accuracy of different approximation functions is quite different.

The main idea of intelligent calculation method is to transform the identification of moving load into an optimization problem, and use the heuristic algorithms or optimization algorithm to solve the problem. For example, Chen et al. [25] developed a modified preconditioned conjugate gradient method for moving force identification by preconditioned conjugate gradient methods with a modified Gram–Schmidt algorithm. Chisari et al. [26] proposed an identification approach based on genetic algorithm. Based

on the firefly algorithm, Pan et al. [27] presented a novel method for moving force identification. Zhou et al. [28] applied least-squares support vector machine to identify the inverse model. Then based on this inverse model, the operational responses were adopted to determine the real-time excitation force. Zhou et al. [29] proposed a novel impact load identification method of nonlinear structures using deep Recurrent Neural Network.

In addition to the above load identification methods, many scholars have also proposed many other methods. For example, Li et al. [30] proposed an online dynamic load identification algorithm based on an extended Kalman filter. Pinkaew [31] proposed the updated static component regularization technique for moving force identification. Yang et al. [32] studied the application of strain influence line method to moving load identification. Qian et al. [33] proposed a novel moving load identification method based on the bending moment influence line. Liu et al. [34] proposed a novel and efficient method utilizing blind source separation and orthogonal matching pursuit. Jiang et al. [35] proposed a novel time-domain algorithm based on the Newmark-b method.

In fact, the direct method is simple, straightforward, and clear, but the MFI results are not reliable when there is measurement error and noise interference. Regularization methods can improve the ill-conditioned problem of load identification. However, the regularization parameter selection needs to be considered. Moreover, the basis function expansion method has the same limitation. The function approximation method is insensitive to noise, but its identification accuracy is excessively dependent on the basic function type. Meanwhile, error accumulation occurs when velocity and acceleration are obtained from the deflection approximated by the function approximation method, which brings the inevitable error to the identification results. Although intelligent calculation methods avoid the shortcomings of the above methods, they require a large amount of data for network training or model construction, which is costly and time consuming, and cannot be used for real-time load identification. According to the discussion above, a new conjugate gradient method is established for MFI of vehicle–bridge system, which is based on the ideas of existing method in [36]. The proposed method does not need to select regularization parameters in advance and model construction and training. Meanwhile, it has the advantages of fast convergence and small storage space which reduces the cost of load identification and improves the speed of load identification. In addition, the iterative process has regularization effect, so the proposed method has anti-noise property. In a word, the proposed method can improve the ill-conditioned problem of load identification and identify the moving load on the bridge efficiently and quickly.

This paper is organized as follows. "Moving Force Identification in Time Domain" section describes the basic theory of the moving load identification of vehicle–bridge system. The modified conjugate gradient (MCG) method is established in "Establishment of Modified Conjugate Gradient Method" section. In "Proof of Global Convergence" section, the global convergence of the MCG method is proved by mathematical theory. The preconditioned technique is introduced in "Theory of Preconditioned Modified Conjugate Gradient (PMCG)" section. Numerical simulations are carried out to investigate the stability and effectiveness of the proposed method in "Numerical Simulation" section. Finally, some conclusions are summarized in "Conclusion" section.

Background of Theory

Moving Force Identification in Time Domain

As shown in Fig. 1, the vehicle–bridge system is modeled as a Bernoulli–Euler simply supported beam subjected to

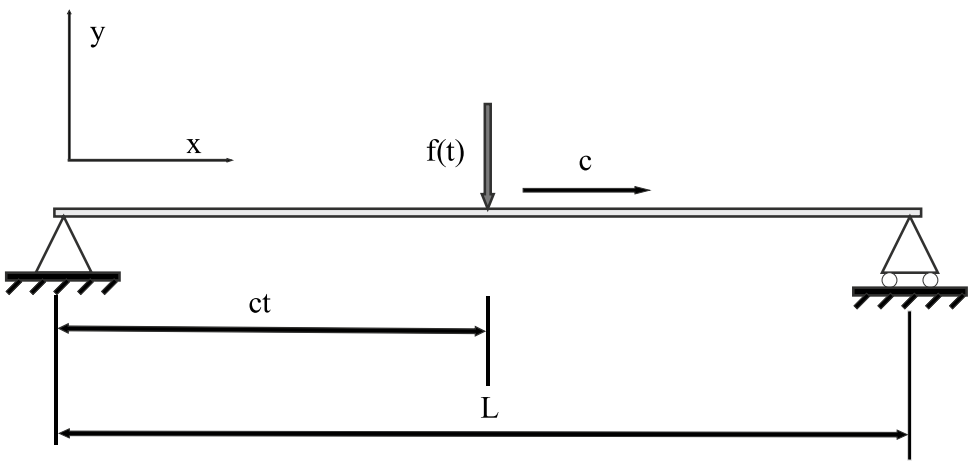

Fig. 1 Moving force identification model with a Bernoulli–Euler simply supported beam

unknown time-varying forces [1]. Assuming that the force $f(t)$ moves from left to right at a constant velocity, the motion equation in terms of the modal coordinate $q_n(t)$ can be written as

$$\ddot{q}_n(t) + 2\xi_n\omega_n\dot{q}_n(t) + \omega_n^2 q_n(t) = \frac{2}{\rho L}p_n(t), \tag{1}$$

where ξ_n is the n-th modal damping ratio; $p_n(t) = f(t)\sin(\frac{n\pi ct}{L})$ is the modal force; ω_n is the $n-th$ modal frequency; ρ is the density of the beam; L is the span of the beam. Based on modal superposition and time-domain deconvolution, the dynamic deflection $v(x, t)$ of the beam at point x and time t can be obtained as

$$\begin{aligned} v(x,t) = \sum_{n=1}^{\infty} \frac{2}{\rho L\omega_n'} \sin\frac{n\pi x}{L} \int_0^t e^{-\xi_n\omega_n(t-\tau)} \\ \sin\left[\omega_n'(t-\tau)\right] \sin\frac{n\pi c\tau}{L} f(\tau)d\tau, \end{aligned} \tag{2}$$

where $\omega_n' = \omega_n\sqrt{(1-\xi_n^2)}$.

The acceleration and bending moment response can be obtained by $v(x, t)$. Then according to the relationship between dynamic response and moving force, which together with the discretization and dimensionless processing, the following equation is formed:

$$Aw = r, \tag{3}$$

where A is the vehicle–bridge system matrix, w is the moving force vector, and r is the dynamic response vector. The specific form of A and r can be referred to [1], which will not be repeated here.

Establishment of Modified Conjugate Gradient Method

It can be seen from "Moving Force Identification in Time Domain" section that the load identification problem is finally transformed into the solution of the high-dimensional equation. To facilitate the calculation, the original equation is usually transformed into the following symmetric positive definite equations

$$Aw = r \Leftrightarrow Kw = b, \tag{4}$$

where $K = A^TA, b = A^Tr$.

By constructing the corresponding objective function, the problem about solving large system of linear equations $Kw = b$ can be transformed into an unconstrained optimization problem

$$\min_{w\in R^n} H(w), \tag{5}$$

where $H(w)$ represents the objective function, which is defined as

$$H(w) = \frac{1}{2}w^TKw - w^Tb. \tag{6}$$

As we all know, the conjugate gradient algorithm is a common optimization method which has the characteristics of small storage space and fast convergence. Therefore, the conjugate gradient method can be used for load identification, and the iteration form can be expressed as

$$w_{i+1} = w_i + \alpha_i d_i, \quad i = 0, 1, 2, \ldots, \tag{7}$$

where α_i is the step length and d_i is the search direction. This step size α_i is often obtained by the Wolfe line search method. The search direction d_i is defined as

$$d_i = \begin{cases} -g_i, & i = 1 \\ -g_i + \beta_i d_{i-1}, & i \geq 2 \end{cases}, \tag{8}$$

where g_i is the gradient of $H(w)$ and β_i is a scalar. Different parameters β_i correspond to different conjugate gradient methods. There are many different conjugate gradient methods, such as HS conjugate gradient [37], RPR conjugate gradient [38], and DY conjugate gradient [39], which are given by $\beta_i^{HS} = \frac{g_i^T(g_i-g_{i-1})}{d_{i-1}^T(g_i-g_{i-1})}$, $\beta_i^{PRP} = \frac{g_i^T(g_i-g_{i-1})}{\|g_{i-1}\|^2}$ and $\beta_i^{DY} = \frac{\|g_i\|^2}{d_{i-1}^T(g_i-g_{i-1})}$, respectively. Different conjugate gradient methods have different properties. In fact, the DY method has good convergence property, and the PRP method and the HS method have good numerical performance. Based on this idea, many new conjugate gradient methods are derived. Such as VHS [40], VRPR [41], and MDY [42], which are given by $\beta_i^{\text{VHS}} = \frac{\|g_i\|^2 - \frac{\|g_i\|}{\|g_{k-1}\|}|g_i^Tg_{i-1}|}{d_{i-1}^T(g_i-g_{i-1})}$, $\beta_i^{\text{VPRP}} = \frac{g_i^T(g_i - \frac{\|g_i\|}{\|g_{i-1}\|}g_{i-1})}{\|g_{i-1}\|^2}$ and $\beta_i^{\text{MDY}} = \frac{g_i^T(g_i - \frac{g_i^Td_{i-1}}{\|d_{i-1}\|^2}d_{i-1})}{d_{i-1}^T(g_i-g_{i-1})}$, respectively.

Based on the analysis above, this paper proposes a modified conjugate gradient method, in which β_i is defined as

$$\beta_i = \begin{cases} \frac{g_i^T(g_i - \mu\frac{d_{i-1}g_i^T}{\|d_{i-1}\|^2}d_{i-1})}{d_{i-1}^T(g_i-g_{i-1})} & g_i^Tg_{i-1} \geq 0, \\ \frac{g_i^T(g_i + \mu\frac{d_{i-1}g_i^T}{\|d_{i-1}\|^2}d_{i-1})}{d_{i-1}^T(g_i-g_{i-1})} & g_i^Tg_{i-1} < 0. \end{cases} \tag{9}$$

where $0 < \mu < 1$ is a variable parameter.

In this paper, the step size α_i is determined by the following standard Wolfe line search

$$H(x_i + \alpha_i d_i) - H(x_i) \leq \delta\alpha_i g_i^T d_i, \tag{10}$$

$$g(x_i + \alpha_i d_i)^T d_i \geq \sigma g_i^T d_i, \tag{11}$$

where $0 < \delta < \sigma < 1$. We can name the conjugate gradient method based on (9–11) as the modified conjugate gradient method.

Throughout the paper, we make the following assumptions:

(AC1): The objective function $H(w)$ has a lower bound on the level set $\Omega = \{w \in R^n | H(w) \le H(w_1)\}$, where w_1 is the initial point.
(AC2): The objective function $H(w)$ is continuously differentiable in some neighborhood U of Ω, in which the gradient is Lipchitz continuous, and that is to say there exists a constant $L > 0$, such that

$$\|g(w) - g(y)\| \le L\|w - y\|, \quad \forall w, y \in \Omega. \tag{12}$$

The new conjugate gradient algorithm is given as follows:

Step 1: Select an initial point $w_1 \in R_n$, set $i := 1, \varepsilon > 0, d_1 = -g_1$; if $\|g_1\| \le \varepsilon$, then stop.
Step 2: Compute the step length α_i by the standard Wolfe line search such that α_i satisfies the formula (10)–(11).
Step 3: Calculate w_{i+1} by the formula (7); if $\|g_{i+1}\| \le \varepsilon$, then stop.
Step 4: Compute β_i by the formula (9), and generate d_{i+1} by the formula (8).
Step 5: Let $i = i + 1$; go to step 2.

Proof of Global Convergence

Lemma 1 *Suppose that* (*AC*1) *and* (*AC*2) *hold. The parameter* β_i *comes from formula* (9), *and let the sequences* g_i *and* d_i *be generated by the new conjugate gradient algorithm. If* $g_i \ne 0$, $\mu \in [0, 1]$ *for* $i \ge 1$, *then* $g_i^T d_i < 0$.

Proof Case (1) if $\mu = 0$, then $\beta_i = \beta_i^{DY}$.

Case (2) if $i = 1$, then $g_1^T d_1 = -\|g_1\|^2 < 0$. The conclusion holds.

Assume that $g_{i-1}^T d_{i-1} < 0$ is true for $i - 1$ and $i \ge 2$, from (11), we have

$$d_{i-1}^T (g_i - g_{i-1}) \ge (\sigma - 1) g_{i-1}^T d_{i-1} > 0. \tag{13}$$

Define η_i as the angle between the g_i and d_{i-1} vectors, then

$$\cos \eta_i = \frac{g_i^T d_{i-1}}{\|g_i\| \|d_{i-1}\|}. \tag{14}$$

If $g_i^T g_{i-1} \ge 0$, then we take the inner product of both sides of (8) with vector g_i^T. According to (9) and (11), we have

$$\begin{aligned}
\frac{\|d_i\|^2}{(g_i^T d_i)^2} &= \frac{\beta_i^2 \|d_{i-1}\|^2}{(g_i^T d_i)^2} - \frac{2}{g_i^T d_i} - \frac{\|g_i\|^2}{(g_i^T d_i)^2} \\
&= \frac{\beta_i^2 \|d_{i-1}\|^2}{(g_i^T d_i)^2} + \frac{1}{\|g_i\|^2} \left(\frac{1}{\|g_i\|} + \frac{\|g_i\|}{g_i^T d_i} \right)^2 \\
&\le \frac{\beta_i^2 \|d_{i-1}\|^2}{(g_i^T d_i)^2} + \frac{1}{\|g_i\|^2}.
\end{aligned} \tag{15}$$

If $g_k^T g_{k-1} < 0$, we have

$$\begin{aligned}
g_i^T d_i &= -\|g_i\|^2 + \beta_i g_i^T d_{i-1} \\
&= -\|g_i\|^2 + \frac{g_i^T \left(g_i - \frac{\mu d_{i-1} g_i^T d_{i-1}}{\|d_{i-1}\|^2} \right)}{d_{i-1}^T (g_i - g_{i-1})} g_i^T d_{i-1} \\
&= \frac{-\|g_i\|^2 d_{i-1}^T g_i + \|g_i\|^2 d_{i-1}^T g_{i-1} + \|g_i\|^2 g_i^T d_{i-1} - \frac{\mu g_i^T d_{i-1} g_i^T d_{i-1}}{\|d_{i-1}\|^2} g_i^T d_{i-1}}{d_{i-1}^T (g_i - g_{i-1})} \\
&= \frac{\|g_i\|^2 d_{i-1}^T g_{i-1} - \mu \|g_i\|^2 \cos^2 \eta_i \cdot g_i^T d_{i-1}}{d_{i-1}^T (g_i - g_{i-1})} \\
&\le \frac{\|g_i\|^2 g_{i-1}^T d_{i-1} (1 - \sigma \mu \cos^2 \eta_i)}{d_{i-1}^T (g_i - g_{i-1})} < 0.
\end{aligned} \tag{16}$$

By mathematical induction, we know that Lemma 1 is true. □

Lemma 2 *Suppose that* (*AC*1) *and* (*AC*2) *hold. If the step length* α_i *satisfies the standard Wolfe line search* (10) *and* (11), *then we have*

$$0 \le \beta_i \le \frac{g_i^T d_i}{g_{i-1}^T d_{i-1}}. \tag{17}$$

Proof From the formula (9) and the angle η_i, we have

$$\beta_i = \frac{\|g_i\|^2 (1 - \mu \cos^2 \eta_i)}{d_{i-1}^T (g_i - g_{i-1})} \ge 0, (g_i^T g_{i-1} \ge 0), \tag{18}$$

$$\beta_i = \frac{\|g_i\|^2 (1 + \mu \cos^2 \eta_i)}{d_{i-1}^T (g_i - g_{i-1})} \ge 0, (g_i^T g_{i-1} < 0). \tag{19}$$

Therefore, $\beta_i \ge 0$.

Exploiting Lemma 1, we obtain

$$\begin{aligned}
\beta_i &= \frac{\|g_i\|^2 (1 - \mu \cos^2 \eta_i)}{d_{i-1}^T (g_i - g_{i-1})} \le \frac{\|g_i\|^2 (1 - \sigma \mu \cos^2 \eta_i)}{d_{i-1}^T (g_i - g_{i-1})} \\
&\le \frac{g_i^T d_i}{g_{i-1}^T d_{i-1}}, (g_i^T g_{i-1} \ge 0),
\end{aligned} \tag{20}$$

$$\begin{aligned}\beta_i =& \frac{\|g_i\|^2(1+\mu\cos^2\eta_i)}{d_{i-1}^T(g_i-g_{i-1})} \le \frac{\|g_i\|^2(1+\sigma\mu\cos^2\eta_i)}{d_{i-1}^T(g_i-g_{i-1})} \\ \le& \frac{g_i^T d_i}{g_{i-1}^T d_{i-1}}, (g_i^T g_{i-1} < 0).\end{aligned} \tag{21}$$

In summary, $\beta_i \le \frac{g_i^T d_i}{g_{i-1}^T d_{i-1}}$. So, $0 \le \beta_i \le \frac{g_i^T d_i}{g_{i-1}^T d_{i-1}}$, and that is to say, Lemma 2 holds. □

Theorem 1 *Suppose that* (*AC*1) *and* (*AC*2) *hold. Considering any iteration of the formula* (8), *where the* d_i *is a descent direction and the step length* α_i *satisfies the standard Wolfe line search conditions, then we have*

$$\sum_{i\ge 1} \frac{(g_i^T d_i)^2}{\|d_i\|^2} < +\infty. \tag{22}$$

Proof From Lemma 1, we have $g_i^T d_i < 0$. By the formula (11), we get

$$d_i^T(g_{i-1}-g_i) \ge (\sigma-1) g_i^T d_i > 0. \tag{23}$$

From (AC2), it follows that

$$d_i^T(g_{i-1}-g_i) \le L\alpha_i \|d_i\|^2. \tag{24}$$

Thus, we can obtain

$$\alpha_i \ge \frac{(\sigma-1) g_i^T d_i}{L\|d_i\|^2}. \tag{25}$$

Because the sequences H_i is monotonic decreasing and convergent, we get

$$\begin{aligned}H_i - H_{i-1} \ge& -\delta\alpha_i g_i^T d_i \ge \frac{-\delta(\sigma-1)(g_i^T d_i)}{L\|d_i\|^2} \\ =& \frac{\delta(1-\sigma)}{L}\frac{(g_i^T d_i)^2}{\|d_i\|^2}.\end{aligned} \tag{26}$$

Taking the limit of the sum of both sides of formula (26), we have

$$\begin{aligned}\sum_{i\ge 1} \frac{\delta(1-\sigma)}{L}\frac{g_i^T d_i^2}{\|d_i\|^2} \le& \sum_{i\ge 1}(H_i - H_{i-1}) \\ =& H_1 - \lim_{x\to\infty} H_i < +\infty.\end{aligned} \tag{27}$$

Therefore, the formula (22) holds, that is, Theorem 1 is true. □

Theorem 2 *Suppose that* (*AC*1) *and* (*AC*2) *hold. The step length* α_i *is generated by the standard Wolfe line search conditions, and Lemma 1 holds.* β_i *is the parameter of the formula* (9). *Then we have*

$$\liminf_{i\to\infty} \|g_i\| = 0. \tag{28}$$

Proof Assume by the contradiction that the formula (28) does not hold. For all i, there exists a constant $\lambda > 0$, such that

$$\|g_i\| \ge \lambda. \tag{29}$$

Rearranging $d_i = -g_i + \beta_i d_{i-1}$ into $d_i + g_i = \beta_i d_{i-1}$, and squaring both sides, we can obtain

$$\|d_i\|^2 = \beta_i^2\|d_{i-1}\|^2 - 2g_i^T d_i - \|g_i\|^2. \tag{30}$$

Dividing the above formula by $(g_i^T d_i)^2$, we get

$$\begin{aligned}\frac{\|d_i\|^2}{(g_i^T d_i)^2} =& \frac{\beta_i^2\|d_{i-1}\|^2}{(g_i^T d_i)^2} - \frac{2}{g_i^T d_i} - \frac{\|g_i\|^2}{(g_i^T d_i)^2} \\ =& \frac{\beta_i^2\|d_{i-1}\|^2}{(g_i^T d_i)^2} + \frac{1}{\|g_i\|^2} - \left(\frac{1}{\|g_i\|} + \frac{\|g_i\|}{g_i^T d_i}\right)^2 \\ \le& \frac{\beta_i^2\|d_{i-1}\|^2}{(g_i^T d_i)^2} + \frac{1}{\|g_i\|^2}.\end{aligned} \tag{31}$$

From the formula (17) of Lemma 2, we have

$$\begin{aligned}\frac{\|d_i\|^2}{(g_i^T d_i)^2} \le& \frac{(g_i^T d_i)^2}{(g_{i-1}^T d_{i-1})^2}\frac{\|d_{i-1}\|^2}{(g_i^T d_i)^2} + \frac{1}{\|g_i\|^2} \\ =& \frac{\|d_{i-1}\|^2}{(g_{i-1}^T d_{i-1})^2} + \frac{1}{\|g_i\|^2}.\end{aligned} \tag{32}$$

From the formula (8), we can get

$$d_1 = -g_1. \tag{33}$$

Thus, we have

$$\frac{\|d_1\|^2}{(g_1^T d_1)^2} = \frac{1}{\|g_1\|^2}. \tag{34}$$

By recursion, we have

$$\frac{\|d_i\|^2}{(g_i^T d_i)^2} \le \sum_{j=1}^{i}\frac{1}{\|g_j\|^2} \le \frac{i}{\lambda^2}. \tag{35}$$

That is,

$$\frac{(g_i^T d_i)^2}{\|d_i\|^2} \ge \frac{\lambda^2}{i}. \tag{36}$$

Summing both sides of the above formula, we can obtain

$$\sum_{i\geq 1}\frac{\left(g_i^T d_i\right)^2}{\left\|d_i\right\|^2}\geq \lambda^2\sum_{i\geq 1}\frac{1}{i}=+\infty. \tag{37}$$

This contradicts (22). So, Theorem 2 holds. □

Theory of Preconditioned Modified Conjugate Gradient (PMCG)

It is well known that conjugate gradient method converges slowly when $cond(K)$ is large. Therefore, the preconditioned technology is introduced to deal with this problem. The main idea of the preconditioned technology is to transform the original problem into an equivalent problem that is easy to solve, and its equivalent transformation is given as follows:

$$Kw=b\Leftrightarrow \widetilde{K}\widetilde{w}=\widetilde{b}, \tag{38}$$

where, $\widetilde{K}=Q^{-1}KQ^{-T}$, $\widetilde{w}=Q^T w$, $\widetilde{b}=Q^{-1}b$. Q represents the preconditioned matrix, and its selection method can be found in [43]. In this paper, the diagonal matrix is chosen as the preconditioned matrix. Through this equivalent transformation, if $cond(\widetilde{K})<cond(K)$, the solving speed of conjugate gradient algorithm will be improved.

Based on MCG algorithm and the preconditioned technology, the PMCG algorithm can be established. The computation flowchart of the PMCG algorithm is shown in Fig. 2. In the following simulation experiment, the convergence control error ε of the conjugate gradient method is set to 10e-5 and the maximum number of iterations *maxiter* is set to 5000.

Numerical Simulation

Problem Description

As shown in Fig. 1, a Bernoulli–Euler simply supported beam subjected to moving force is investigated to evaluate the performances of the proposed algorithm in this paper. The beam has a span of 40 m, and the parameters of the beam are given as: the flexural rigidity $EI=1.274916\times 10^{11}\,\mathrm{N\,m^2}$; the density of unit length $\rho=12{,}000\,\mathrm{kg\,m^{-1}}$; the first three natural frequencies of the beam are 3.2 Hz, 12.8 Hz and 28.8 Hz, respectively. The parameters of the vehicle are given as follows: the speed of vehicle moving is $40\,\mathrm{m\,s^{-1}}$; the distance between two axles is 4 m. The analysis frequency ranges from 0 to 40 Hz. The sampling frequency is selected as 200 Hz.

Biaxial time-varying force identification with six different cases is investigated. The moving force is given as follows:

$$\begin{aligned}F_1(t)&=20[1+0.1\sin(8\pi t)+0.05\sin(20\pi t)](kN),\\ F_2(t)&=20[1-0.1\sin(8\pi t)+0.05\sin(24\pi t)](kN).\end{aligned} \tag{39}$$

There are measurement error and noise interference in the practical engineering, so the polluted responses with the random noise are given as

$$b_{\mathrm{simulate}}=b_{\mathrm{true}}(1+nl\times N_{\mathrm{noise}}), \tag{40}$$

where, b_{true} is the real response of simulation; b_{simulate} represents the polluted measured response; nl represents the noise level, which is selected as 0–20% in subsequent studies; N_{noise} is the random white Gaussian noise.

The acceleration and bending moment sensors are located at 1/4, 1/2, and 3/4 of the bridge span, respectively. For convenience, $M14$ represents the bending moment response of 1/4 bridge span, $J12$ represents the acceleration response of 1/2 bridge span, and so on. The load identification speed will be evaluated by the number of iterations. The relative percentage error (RPE) is adopted as the criterion to evaluate the accuracy of load identification, and the calculation formula is given as

$$RPE=\frac{\left\|f_{\mathrm{iden}}-f_{\mathrm{true}}\right\|}{\left\|f_{\mathrm{true}}\right\|}\times 100\%, \tag{41}$$

where f_{true} represents the true load; f_{iden} represents the load from MFI.

Parameter Selection

As can be seen from the description in "Background of Theory" section, there is a variable parameter μ in the PMCG method, which needs to be selected appropriately. The parameter μ is usually selected by the posterior RPE criterion, which can be described as:

$$\mathrm{RPE}(\mu_{\mathrm{optimal}})=\min_{0<\mu<1}\{\mathrm{RPE}(\mu)\}, \tag{42}$$

where $\mathrm{RPE}(\mu)$ represents the relative percentage error of the identified load by PMCG when the variable parameter is μ, which is defined as follows:

$$\mathrm{RPE}(\mu)=\frac{\left\|F_{\mu,\mathrm{identification}}-F_{\mathrm{true}}\right\|}{\left\|F_{\mathrm{true}}\right\|}, \tag{43}$$

where $F_{\mu,\mathrm{identification}}$ represents the load identified by the PMCG method when the parameter is μ, and F_{true} represents the true load.

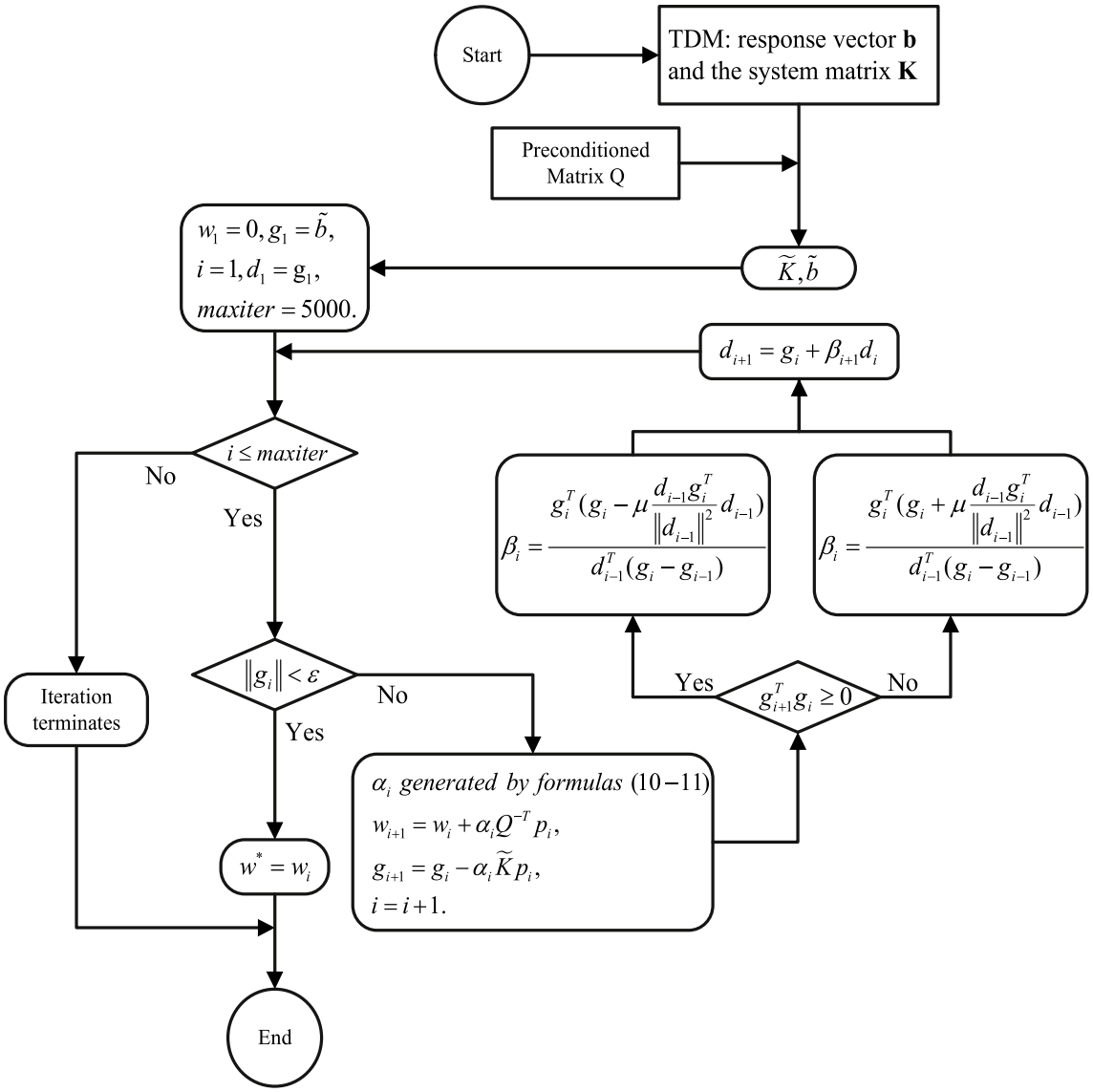

Fig. 2 The flowchart of the PMCG algorithm

However, in practical engineering, the true load F_{ture} required in RPE criterion is generally unknown. Therefore, a new equivalent evaluation criterion named as response relative percentage error (RRPE) can be adopted, and it can be expressed as

$$\text{RRPE}(\mu_{\text{optimal}}) = \min_{0<\mu<1}\{\text{RRPE}(\mu)\}, \tag{44}$$

where $\text{RRPE}(\mu)$ represents the relative percentage error between the measured response and the reconstructed response when the parameter is μ, which can be expressed as:

$$\text{RRPE}(\mu) = \frac{\left\|R_{\mu,\text{reconstruction}} - R_{\text{measurement}}\right\|}{\left\|R_{\text{measurement}}\right\|}, \tag{45}$$

where $R_{\text{measurement}}$ represents the measured response, and $R_{\mu,\text{reconstruction}}$ represents the reconstructed response from the load identified by the PMCG when the parameter is μ.

For the iterative method, the number of iterations has a linear relationship with the identification speed. Therefore, it is necessary to take the number of iterations as the evaluation criterion, and its mathematical expression is given as

$$Iterations(\mu_{\text{optimal}}) = \min_{0<\mu<1}\{Iterations(\mu)\}, \tag{46}$$

where *Iterations*(μ) represents the number of iterations when the parameter is μ.

The sensor configuration is selected as M14 &M12 &M34 &J14 &J12 &J34, and the parameters are chosen by the above two posterior parameter selection criteria under five different noise levels. The number of iterations of load identification corresponding to different μ is shown in Fig. 3. It can be seen from Fig. 3 that the iteration number of PMCG is relatively low when μ is between 0.87 and 0.99. Similarly, the relative percentage error of the reconstruction response corresponding to different μ is shown in Fig. 4. As can be seen from Fig. 4, when μ is between 0.84 and 0.99, the reconstruction response of load identified by PMCG is more consistent with the measured response. It can be seen from the above description that when the variable parameter μ is between 0.87 and 0.99, PMCG has good numerical performances and convergence, so the variable parameter μ is selected as 0.98 in the following analysis.

Moving Force Identification and Results Analysis

The accuracy of load identification is affected by the measurement error and noise, so it is necessary to study the anti-noise ability of the proposed algorithm. Generally, the identification error is used to assess the accuracy of load identification results. To verify the accuracy of the proposed PMCG, 6 different sensor configurations are selected to perform load identification under 21 different noise levels, and PMCG is compared with 6 different preconditioned conjugate gradient methods. Figures 5 and 6 show the RPE

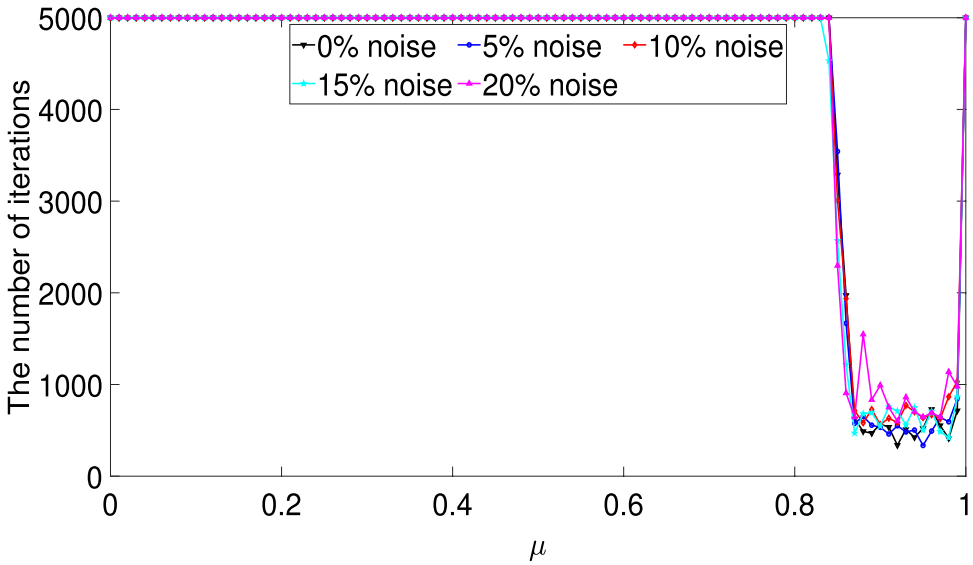

Fig. 3 The iteration number criterion

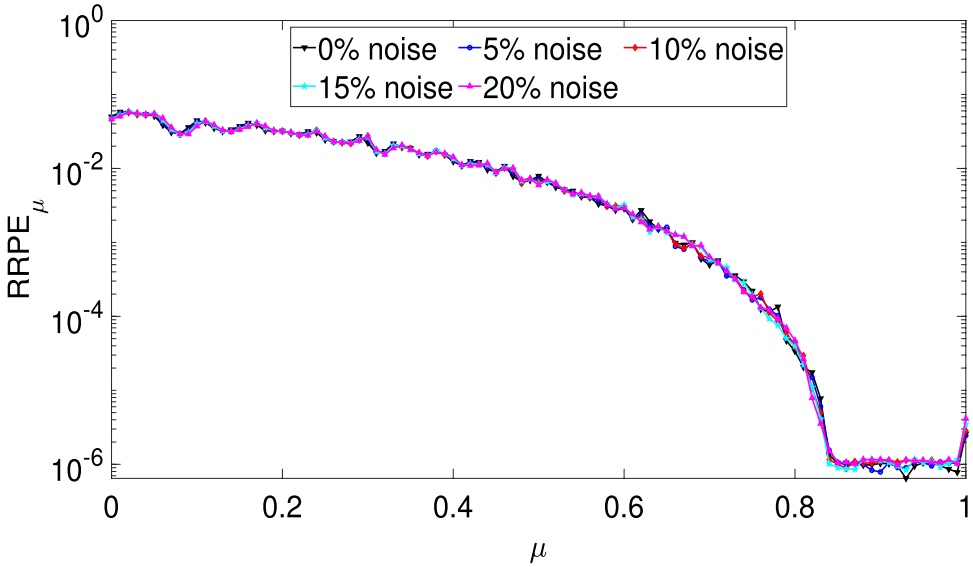

Fig. 4 Reconstructed response relative percentage error criterion

of front and rear axle loads identified by seven methods respectively. It can be seen from Fig. 5 that the errors of PMCG, perconditioned modified DY conjugate gradient (PMDYCG), and perconditioned HS conjugate gradient (PHSCG) in identifying the front axle load are very close under various noise and different sensor configurations. Meanwhile, in most cases, the errors of PMCG, PMDYCG, and PHSCG are lower than those of other four methods. The identification error of seven methods increases with the increase of noise, but the error of PMCG, PMDYCG, and PHSCG increases less than that of the other four methods. Similarly, the same conclusion can be drawn from Fig. 6.

For the iterative method, the number of iterations has a linear relationship with the calculation time, so it is necessary to reduce the number of iterations for real-time load identification. Meanwhile, reducing the number of iterations can effectively decrease the cost of MFI. The number of iterations of seven methods in different sensor configurations and with different noise levels is shown in Fig. 7. It can be observed in Fig. 7 that the number of iterations of

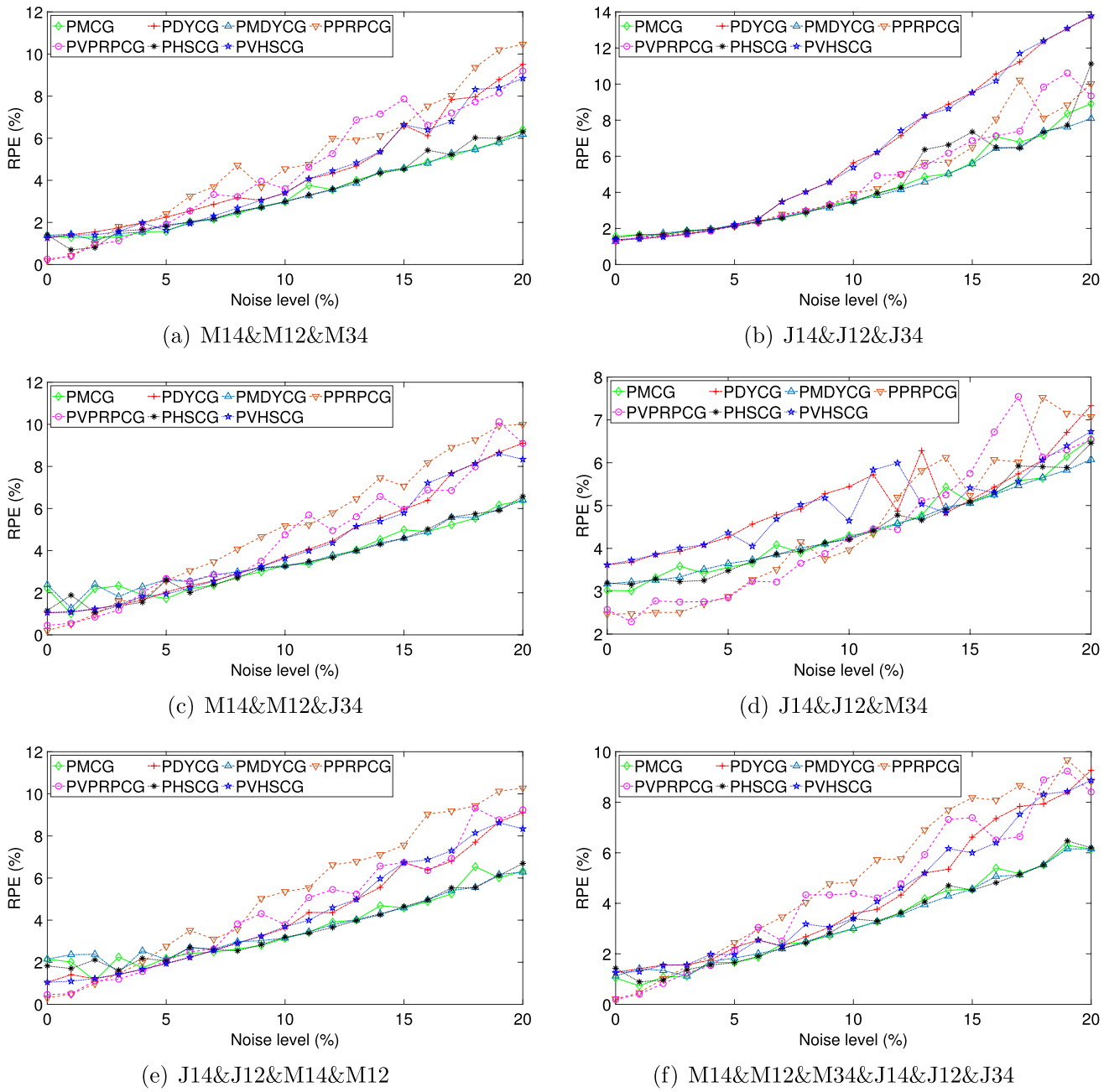

(a) M14&M12&M34

(b) J14&J12&J34

(c) M14&M12&J34

(d) J14&J12&M34

(e) J14&J12&M14&M12

(f) M14&M12&M34&J14&J12&J34

Fig. 5 Comparison on RPE of front axle loads identified by seven methods under different sensor placement

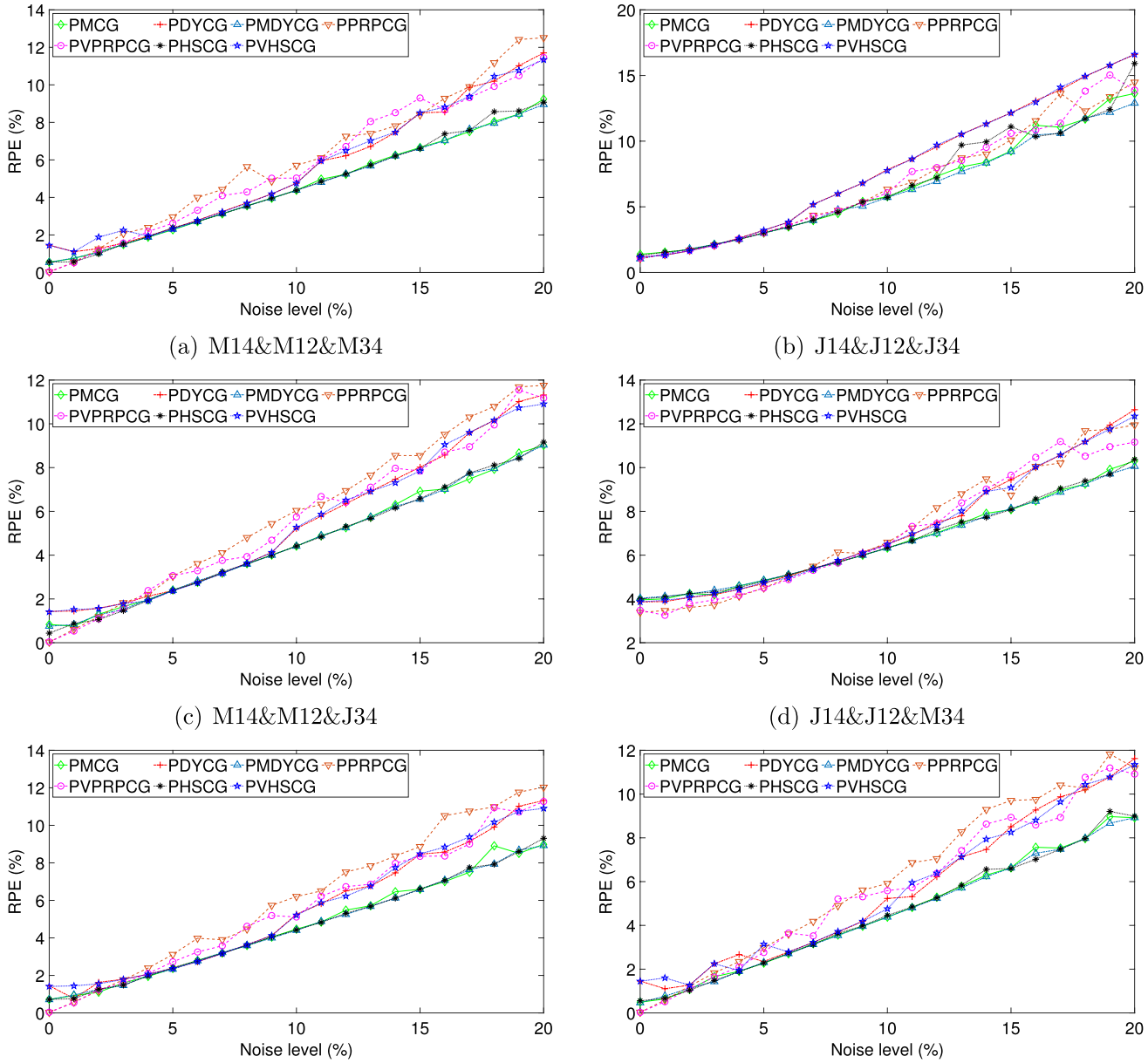

Fig. 6 Comparison on RPE of rear axle loads identified by seven methods under different sensor placement

perconditioned DY conjugate gradient (PDYCG) and perconditioned VHS conjugate gradient (PVHSCG) methods is significantly lower than those of the other five methods, which indicate that the convergence speed of PDYCG and PVHSCG is much faster than that of other methods. Conversely, the number of iterations of the perconditioned PRP conjugate gradient (PPRPCG) and perconditioned VPRP conjugate gradient (PVPRPCG) almost reaches the preset maximum (5000). In addition, it can be obviously seen that the number of iterations of PMCG method is lower than PMDYCG and PHSCG.

Table 1 lists the average number of iterations and average identification errors of 7 methods under 21 different noise levels. In this table, the last row is the average number of iterations and the mean error of the biaxial load identification for all the above sensors configurations and all the noise situations. As can be seen from Table 1, PDYCG and PVHSCG have the least average number of iterations, which indicates that their identification speed is fast. The average error of PMCG, PMDYCG, and PHSCG is small, which indicates that their identification accuracy is good. Based on the results in Table 1, it can be seen that compared with

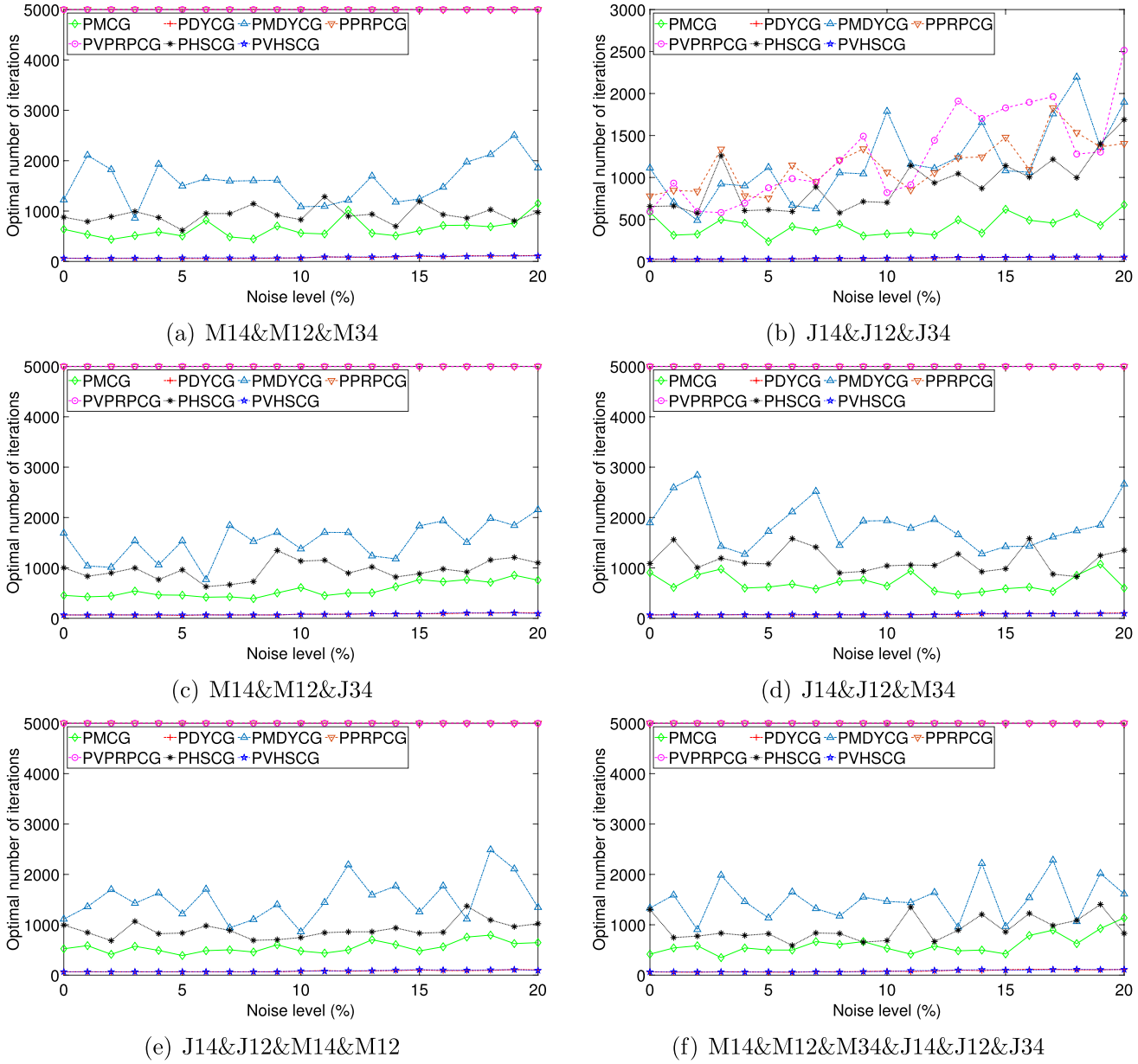

Fig. 7 Comparison on the number of iterations of MFI by seven methods under different sensor placement

PMDYCG and PHSCG, the average number of iterations of PMCG is reduced by about 62.37% and 39.95%, respectively; compared with PDYCG and PVHSCG, the front axle load identification errors of PMCG are decreased by 20.82% and 20.23%, and the rear axle load identification error of PMCG is decreased by 15.31% and 15.79%, respectively; compared with PPRPCG and PVPRPCG, the average number of iterations of PMCG is reduced by 86.77% and 86.77%, the front axle load identification errors are reduced by 24.29% and 16.53%, and the rear axle load identification errors are reduced by 18.10% and 13.52%, respectively. The above data analysis shows that the PMCG method reduces the average number of iterations and improves the speed of load identification on the premise of ensuring the identification accuracy.

Figure 8 shows the comparison between the true load and the identified load by seven methods from the combined responses ($M14\&M12\&M34\&J14\&J12\&J34$). As

Table 1 The comparison of the average number of iterations and average identification RPE (%)

Location	Method	PMCG	PDYCG	PMDYCG	PPRPCG	PVPRPCG	PHSCG	PVHSCG
M14 &M12 &M34	Front axle	3.27	4.31	3.26	4.89	4.46	3.29	4.13
	Rear axle	4.52	5.46	4.49	6.01	5.63	4.55	5.51
	Iterations	644	80	1588	5000	5000	926	84
J14 &J12 &J34	Front axle	4.17	6.26	4.02	4.66	4.66	4.43	6.25
	Rear axle	6.46	8.01	6.25	6.86	6.9	6.71	8.02
	Iterations	429	39	1188	1149	1261	919	39
M14 &M12 &J34	Front axle	3.52	4.21	3.63	5.06	4.47	3.43	4.18
	Rear axle	4.57	5.47	4.55	5.95	5.54	4.54	5.45
	Iterations	562	80	1533	5000	5000	958	81
J14 &J12 &M34	Front axle	4.45	5.07	4.39	4.51	4.4	4.42	4.97
	Rear axle	6.59	7.19	6.57	7.15	7.03	6.61	7.15
	Iterations	701	78	1863	5000	5000	1146	79
J14 &J12 &M14 &M12	Front axle	3.55	4.19	3.62	5.25	4.46	3.53	4.22
	Rear axle	4.61	5.43	4.55	6.12	5.54	4.56	5.46
	Iterations	553	80	1501	5000	5000	900	82
M14 &M12 &M34 &J14 &J12 &J34	Front axle	3.27	4.05	3.22	5	4.18	3.34	4.12
	Rear axle	4.54	5.4	4.51	6.13	5.53	4.6	5.57
	Iterations	585	81	1560	5000	5000	938	84
Average	Front axle	3.71	4.68	3.69	4.89	4.44	3.74	4.65
	Rear axle	5.22	6.16	5.15	6.37	6.03	5.26	6.19
	Iterations	579	73	1539	4358	4377	964	75

shown in Fig. 8, when the noise level is 0%, all seven methods can accurately identify the moving load. When the noise level increases to 5%, seven methods can identify the load, but all of them have a slight deviation. When the noise level increases to 10%, all the seven methods have large error, but the identification error of PMCG, PDYCG, PMDYCG, and PHSCG is, respectively, smaller than PVPRPCG, PPRPCG, and PVHSCG. When the noise level reaches the extreme value 20%, the identification error of PMCG, PMDYCG, and PHSCG is less than that of PDYCG, PPRPCG, PVPRPCG, and PVHSCG. The above results also demonstrate that PMCG, PMDYCG, and PHSCG have high identification accuracy and strong robustness.

Spectrum Analysis

As we all know, the moving load is a special dynamic load whose main dynamic characteristics contain frequency and corresponding amplitude. To verify the accuracy of PMCG in identifying the moving loads, the spectrum analysis is

Table 2 The comparison of amplitude and ARPE (%)

Noise level	Load component	Static		Low-frequency		High-frequency	
		Amplitude	ARPE	Amplitude	ARPE	Amplitude	ARPE
0% noise	Front axle	20.01	**0.05**	1.999	**0.05**	0.8794	**12.06**
	Rear axle	20	**0**	1.999	**0.05**	0.9041	**9.59**
5% noise	Front axle	19.96	**0.25**	1.89	**5.45**	0.8741	**12.59**
	Rear axle	20.09	**0.45**	2.101	**5.10**	0.8522	**14.78**
10% noise	Front axle	19.93	**0.35**	1.783	**10.85**	0.7117	**28.83**
	Rear axle	20.19	**0.95**	2.205	**10.25**	0.6608	**33.92**
15% noise	Front axle	19.88	**0.65**	1.674	**16.30**	0.6847	**31.53**
	Rear axle	20.29	**1.45**	2.308	**15.40**	0.6072	**39.28**
20% noise	Front axle	19.85	**0.75**	1.567	**21.65**	0.6073	**39.27**
	Rear axle	20.38	**1.90**	2.413	**20.65**	0.504	**49.60**

The bold part represents the amplitude error; static, Low-frequency and High-frequency component corresponding to exact amplitude is 20 kN, 2 kN and 1kN, respectively

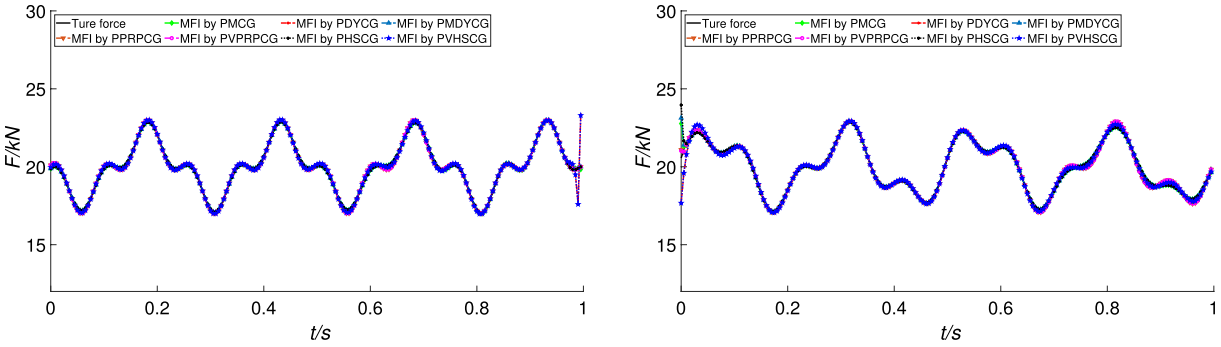

(a) Front axle with 0% noise

(b) Rear axle with 0% noise

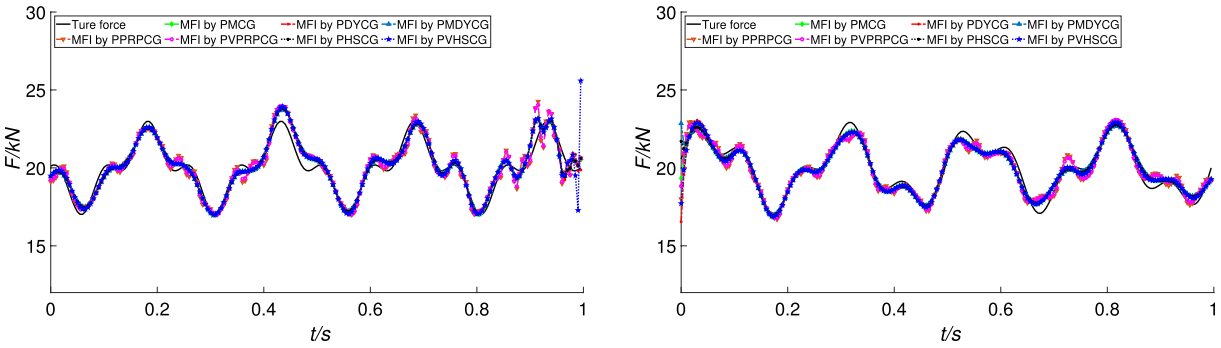

(c) Front axle with 5% noise

(d) Rear axle with 5% noise

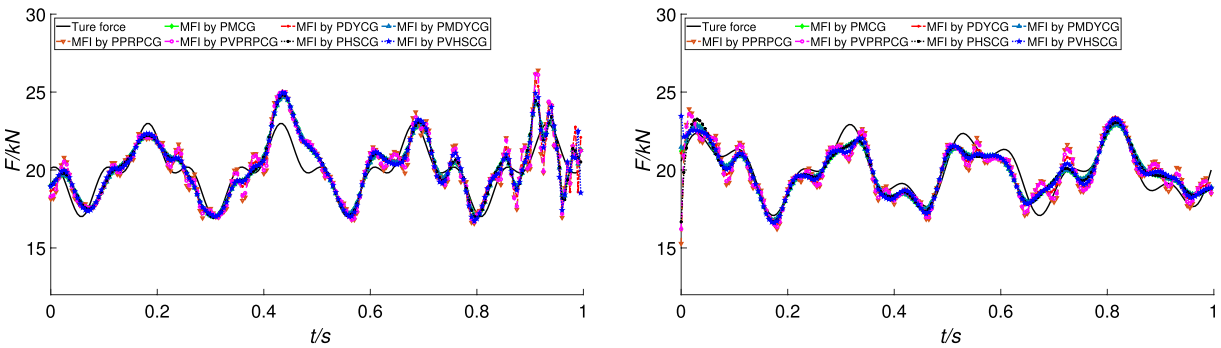

(e) Front axle with 10% noise

(f) Rear axle with 10% noise

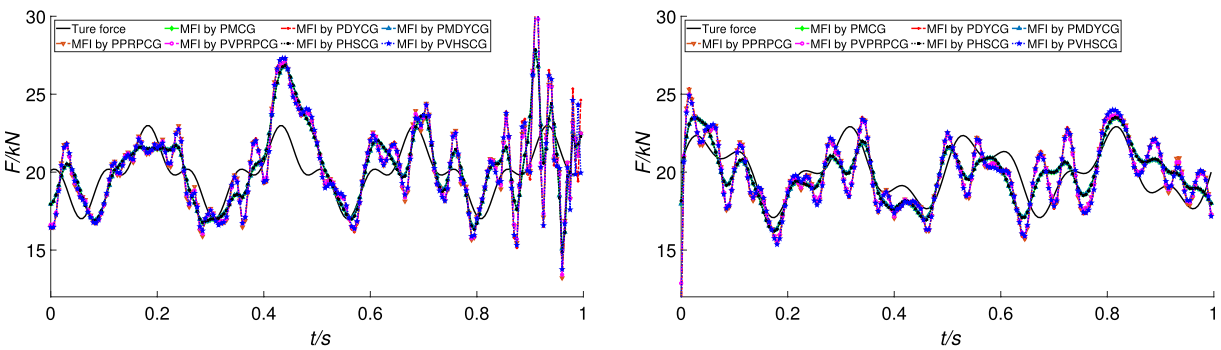

(g) Front axle with 20% noise

(h) Rear axle with 20% noise

Fig. 8 The identification results of seven methods under different noise levels

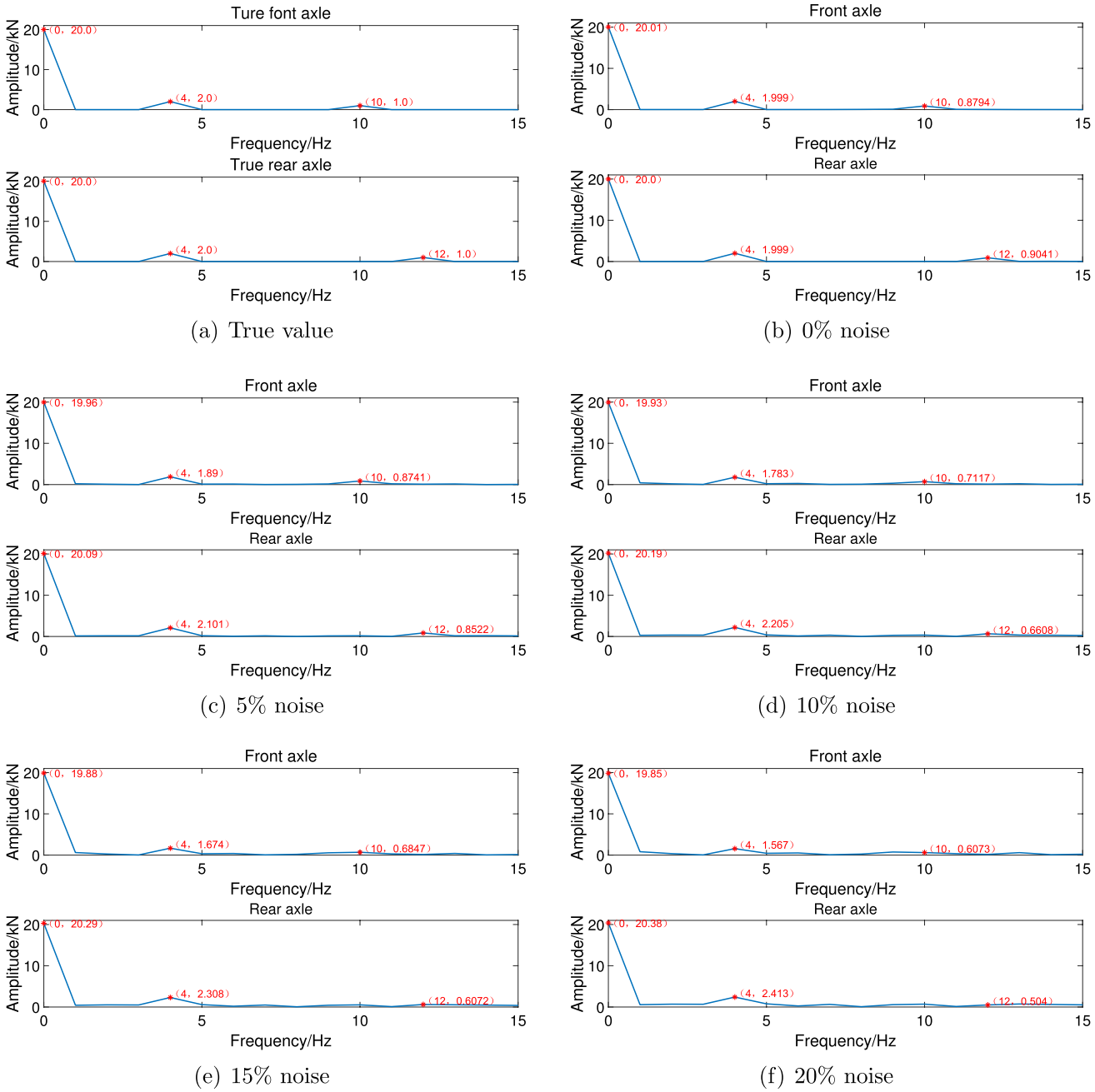

Fig. 9 The frequency spectrogram of the identified loads by PMCG under different noise levels

carried out to study the moving loads identified by PMCG. First, the dynamic characteristics (frequency and amplitude) of simulated true loads and the identified loads are obtained by frequency spectrum analysis. Then the amplitude relative percentage error (ARPE) between the load identified by PMCG and the exact values is caculated by:

$$ARPE = \frac{\left\|A_{\text{identification}} - A_{\text{true}}\right\|}{\left\|A_{\text{true}}\right\|} \times 100\% \tag{47}$$

where $A_{\text{identification}}$ represents the amplitude of the load identified by PMCG, and A_{true} represents the exact values.

The sensor configuration is selected as $M14\&M12\&M34\&J14\&J12\&J34$. The moving loads are identified by PMCG under five different noise levels, and the spectral analysis of the loads is also performed. The spectrum analysis diagram is shown in Fig. 9, and the amplitude corresponding to the principal frequency and amplitude errors is shown in Table 2, and the relationship

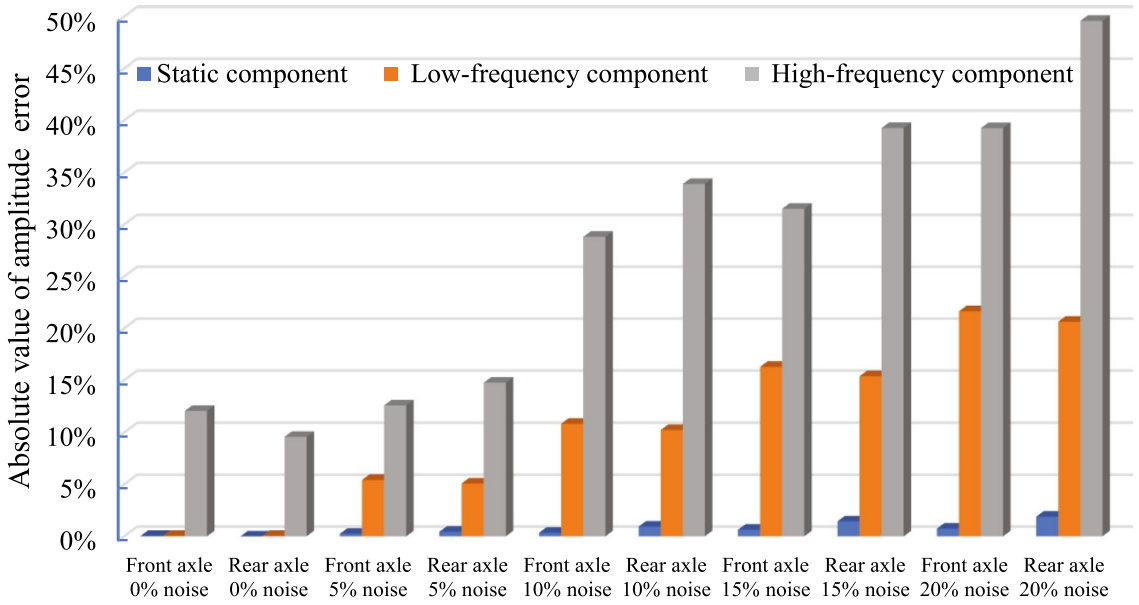

Fig. 10 Relationship between APRE of each frequency component and noise

between the ARPE of each frequency component and noise is shown in Fig. 10. According to Fig. 9, when the noise level is 0%, PMCG can accurately obtain the main frequency and the corresponding amplitude of the moving load. As the noise level increases from 0 to 10%, PMCG can accurately obtain the main frequency, but the corresponding amplitude error of the main frequency increases gradually. When the noise level increases to 15%, PMCG can also obtain the main frequency characteristic, and the corresponding amplitude error increases further. At the same time, the appearance of other frequency components interferes with the identification of high-frequency components of moving loads. When the noise level increases to 20%, the static component can still be identified accurately, and the amplitude error of the low-frequency component increases further, but the high-frequency component cannot be identified. It can be found more clearly from Table 2 and Fig. 10 that PMCG can accurately identify the static component of the biaxial load under various noise levels; the amplitude error of low-frequency component is linear with noise; the amplitude error of high-frequency component also has a linear relationship with noise, but the slope is large, and the error increases faster. Even in the absence of noise, the amplitude identification accuracy of high-frequency components is low.

Conclusion

A new PMCG algorithm based on improved gradient operator and preconditioned technology is proposed for MFI of bridge structure. The time-domain deconvolution technology and modal superposition method transform the moving load identification problem into the solution of large linear equations problem. Then it is transformed into an equivalent linear equations problem by the preconditioned technology. Finally, the moving load identification problem is solved by the proposed conjugate gradient method. Meanwhile, the identification situation of different load components is studied by the frequency spectrum analysis method. Numerical simulations are carried out for the verification of the proposed method. Some conclusions can be given as follows:

1. Compared with the preconditioned conjugate gradient method with good convergence property, such as PDYCG and PVHSCG, PMCG has higher identification accuracy. Compared with the conjugate gradient method with good numerical performance, such as PMDYCG and PHSCG, PMCG reduces the number of optimization iterations and improves the identification speed of moving load identification on the premise of ensuring accuracy.

2. For sensor configuration, only using acceleration responses as the input responses of load identification can achieve fast identification, but the identification accuracy is low. Using the combination of acceleration and bending moment responses as the input responses of load identification can accurately identify the moving load.
3. As for the different frequency components of moving loads, PMCG has high identification accuracy for static and low-frequency components of loads, and the amplitude deviation of low-frequency components is linear with the noise level. Under the condition of low noise level, the low-frequency components can be accurately obtained, which can be used for dynamic weighing of low-frequency moving loads.

In the future, we will apply the proposed algorithm into more complex moving load identification problems with viscoelastic boundary conditions and different ground foundation conditions. To verify the feasibility of practical engineering application of the proposed algorithm, experimental verification will be performed in the next step working.

Acknowledgements Funding was provided by National Natural Science Foundation of China (Grant No. 51975324) and Open Fund of Hubei key Laboratory of Hydroelectric Machinery Design and Maintenance (Grant No. 2019KJX12).

References

1. Law SS, Chan THT, Zeng QH (1997) Moving force identification: a time domain method. J Sound Vib 201(1):1–22
2. Huang LX, Deng ZC, Hou XH (2008) Precision analysis for dynamic moving load identification of bridge structure based on precise integration method. J Hebei Univ Sci Technol 29(2):124–127 ((**In Chinese**))
3. Hou XH, Deng ZC, Huang LX (2008) An improved symplectic precise integration method for moving load identification of bridge structure. J Dyn Control 6(01):66–71 (**in Chinese**)
4. Liu J, Meng XH, Jiang C, Han X, Zhang DQ (2016) Time-domain Galerkin method for dynamic load identification. Int J Numer Methods Eng 105:620–640
5. Uhl T (2007) The inverse identification problem and its technical application. Arch Appl Mech 77(5):325–337
6. Qiao GD, Rahmatalla S (2021) Moving load identification on Euler–Bernoulli beams with viscoelastic boundary conditions by Tikhonov regularization. Inverse Probl Sci Eng 29(8):1070–1107
7. Wang NJ, Ren CP, Liu CS (2018) A novel fractional Tikhonov regularization coupled with an improved super-memory gradient method and application to dynamic force identification problems. Math Probl Eng 1:1–16
8. Liu CS, Ren CP (2019) Identification method of cutting coal and rock load based on improved fractional Tikhonov regularization. J China Coal Soc 44(01):332–339 (**in Chinese**)
9. Chen Z, Chan THT (2017) A truncated generalized singular value decomposition algorithm for moving force identification with ill-posed problems. J Sound Vib 401:297–310
10. Chen Z, Qin LF, Zhao SB, Chan THT, Nguyen A (2019) Toward efficacy of piecewise polynomial truncated singular value decomposition algorithm in moving force identification. Adv Struct Eng 22(12):2687–2698
11. Chen Z, Chan THT, Nguyen A, Yu L (2019) Identification of vehicle axle loads from bridge responses using preconditioned least square QR-factorization algorithm. Mech Syst Signal Process 128:479–496
12. Chen Z, Qin LF, Chan THT, Yu L (2021) A novel preconditioned range restricted GMRES algorithm for moving force identification and its experimental validation. Mech Syst Signal Process 155:107635
13. Pan CD, Huang ZJ, You JD, Li YS, Yang LH (2021) Moving force identification based on sparse regularization combined with moving average constraint. J Sound Vib 515:116496
14. Qiao BJ, Zhang XW, Wang CX, Zhang H, Chen XF (2016) Sparse regularization for force identification using dictionaries. J Sound Vib 368:71–86
15. He ZC, Zhang ZM, Li E (2019) Multi-source random excitation identification for stochastic structures based on matrix perturbation and modified regularization method. Mech Syst Signal Process 119:266–292
16. Feng W, Li QF, Lu QH (2020) Force localization and reconstruction based on a novel sparse Kalman filter. Mech Syst Signal Process 144:106890
17. Wang LG, Zhang Q, Sun YL, Qing XR (2020) Moving load identification for STS cranes based on hybrid weighted regularization method. J Phys Conf Ser 1549(04):042109
18. Qiao BJ, Zhang XW, Luo XJ, Chen XF (2015) A force identification method using cubic B-spline scaling functions. J Sound Vib 337:28–44
19. Qiao BJ, Chen XF, Luo XJ, Xue XF (2015) A novel method for force identification based on the discrete cosine transform. J Vib Acoust 137(5):051012
20. Qiao BJ, Luo XJ, Chen XF, Xue XF, Liu RN (2015) The application of cubic B-spline collocation method in impact force identification. Mech Syst Signal Process 64:413–427
21. Liu J, Sun XS, Han X, Jiang C, Yu DJ (2015) Dynamic load identification for stochastic structures based on Gegenbauer polynomial approximation and regularization method. Mech Syst Signal Process 56–57:35–54
22. Liu J, Cao L, Jiang C, Ni B, Zhang D (2020) Parallelotope-formed evidence theory model for quantifying uncertainties with correlation. Appl Math Model 77:32–48
23. Yuan XR, Bu JQ, Man HG, Gao YL (2000) Function approaching method in moving load identification. J Vib Shock 19(01):58–70 (**in Chinese**)
24. Jiang ZG, Sun YR (2006) Application of cubic spline function to moving load identification on a bridge. J Vib Shock 25(06):124–126 (**in Chinese**)
25. Chen Z, Chan THT, Nguyen A (2018) Moving force identification based on modified preconditioned conjugate gradient method. J Sound Vib 423:100–117
26. Chisari C, Bedon C, Amadio C (2015) Dynamic and static identification of base-isolated bridges using genetic algorithms. Eng Struct 102:80–92
27. Pan CD, Yu L (2014) Moving force identification based on firefly algorithm. Adv Mat Res 919–921:329–333
28. Zhou P, Xin JH, Ding JC (2021) Least squares support vector machine method for load identification of nonlinear systems. J Noise Vib Control 41(05):9–37 (**in Chinese**)
29. Zhou JM, Dong LL, Guan W, Yan J (2019) Impact load identification of nonlinear structures using deep recurrent neural network. Mech Syst Signal Process 133:106292

30. Li HQ, Jiang JH, Mohamed MS (2021) Online dynamic load identification based on extended Kalman filter for structures with varying parameters. Symmetry 13(8):1372
31. Pinkaew T (2006) Identification of vehicle axle loads from bridge responses using updated static component technique. Eng Struct 28(11):1599–1608
32. Yang J, Hou P, Yang CQ, Zhang Y (2021) Study on the method of moving load identification based on strain influence line. Appl Sci 11(02):853
33. Qian CZ, Chen CP, Xiao YG (2014) Identification method for moving loads over continuous beam based on bending moment influence lines. Appl Mech Mater 638–640:1079–1084
34. Liu J, Li K (2021) Sparse identification of time-space coupled distributed dynamic load. Mech Syst Signal Process 148:107177
35. Jiang JH, Ding M, Li J (2021) A novel time-domain dynamic load identification numerical algorithm for continuous systems. Mech Syst Signal Process 160:107881
36. Zhu ZB, Zhang DD, Wang S (2020) Two modified DY conjugate gradient methods for unconstrained optimization problems. Appl Math Comput 373:125004
37. Hestenes M, Stifel E (1952) Methods of conjugate gradients for solving linear systems. J Res Nat Bur Stand 49:409–435
38. Polyak BT (1969) The conjugate gradient method in extremal problems. USSR Comput Math Math Phys 9(04):94–112
39. Dai YH, Yuan YX (1999) A nonlinear conjugate gradient method with a strong global convergence property. SIAM J Optim 10(01):177–182
40. Yao SW, Wei ZX, Huang H (2007) A note about WYL's conjugate gradient method and its applications. Appl Math Comput 191(02):381–388
41. Wei ZX, Yao SW, Liu LY (2006) The convergence properties of some new conjugate gradient methods. Appl Math Comput 183(2):1341–1350
42. Huang H (2014) A new conjugate gradient method for nonlinear unconstrained optimization problems. J Henan Univ (Nat Sci) 44(02):141–145 (**in Chinese**)
43. Fan XT, Ji GM (2003) Preconditioned matrix and its structure technique. J Chengdu Univ Technol (Sci Technol Ed) 30(04):432–435 (**in Chinese**)